Interaction of 1,2,5-Chalcogenadiazole Derivatives with Thiophenolate: Hypercoordination with Formation of Interchalcogen Bond versus Reduction to Radical Anion

ARTICLE *in* THE JOURNAL OF PHYSICAL CHEMISTRY A · MAY 2011

Impact Factor: 2.69 · DOI: 10.1021/jp2019523 · Source: PubMed

THE JOURNAL OF PHYSICAL CHEMISTRY A

ARTICLE

pubs.acs.org/JPCA

Interaction of 1,2,5-Chalcogenadiazole Derivatives with Thiophenolate: Hypercoordination with Formation of Interchalcogen Bond versus Reduction to Radical Anion

Elizaveta A. Suturina,[†,‡] Nikolay A. Semenov,[§] Anton V. Lonchakov,[†,‡] Irina Yu. Bagryanskaya,[§] Yuri V. Gatilov,[§] Irina G. Irtegova,[§] Nadezhda V. Vasilieva,[§] Enno Lork,[∥] Rüdiger Mews,*[,∥] Nina P. Gritsan,*[,†,‡] and Andrey V. Zibarev*[,§,‡]

[†]Institute of Chemical Kinetics and Combustion, Siberian Branch of the Russian Academy of Sciences, 630090 Novosibirsk, Russia

[‡]Department of Physics, National Research University—Novosibirsk State University, 630090 Novosibirsk, Russia

[§]Institute of Organic Chemistry, Siberian Branch of the Russian Academy of Sciences, 630090 Novosibirsk, Russia

[∥]Institute for Inorganic and Physical Chemistry, University of Bremen, 28334 Bremen, Germany

Supporting Information

ABSTRACT: According to the DFT calculations, [1,2,5]-thiadiazolo[3,4-*c*][1,2,5]thiadiazole (**4**), [1,2,5]selenadiazolo-[3,4-*c*][1,2,5]thiadiazole (**5**), 3,4-dicyano-1,2,5-thiadiazole (**6**), and 3,4-dicyano-1,2,5-selenadiazole (**7**) have nearly the same positive electron affinity (EA). Under the CV conditions they readily produce long-lived π-delocalized radical anions (π-RAs) characterized by EPR. Whereas **4** and **5** were chemically reduced into the π-RAs with thiophenolate (PhS^-), **6** did not react and **7** formed a product of hypercoordination at the Se center (**9**) isolated in the form of the thermally stable salt [K(18-crown-6)][**9**] (**10**). The latter type of reactivity has never been observed previously for any 1,2,5-chalcogenadiazole derivatives. The X-ray structure of salt **10** revealed that the Se—S distance in the anion **9** (2.722 Å) is ca. 0.5 Å longer than the sum of the covalent radii of these atoms but ca. 1 Å shorter than the sum of their van der Waals radii. According to the QTAIM and NBO analysis, the Se—S bond in **9** can be considered a donor—acceptor bond whose formation leads to transfer of ca. 40% of negative charge from PhS^- onto the heterocycle. For various PhS^-/1,2,5-chalcogenadiazole reaction systems, thermodynamics and kinetics were theoretically studied to rationalize the interchalcogen hypercoordination vs reduction to π-RA dichotomy. It is predicted that interaction between PhS^- and 3,4-dicyano-1,2,5-telluradiazole (**12**), whose EA slightly exceeds that of **6** and **7**, will lead to hypercoordinate anion (**17**) with the interchalcogen Te—S bond being stronger than the Se—S bond observed in anion **9**.

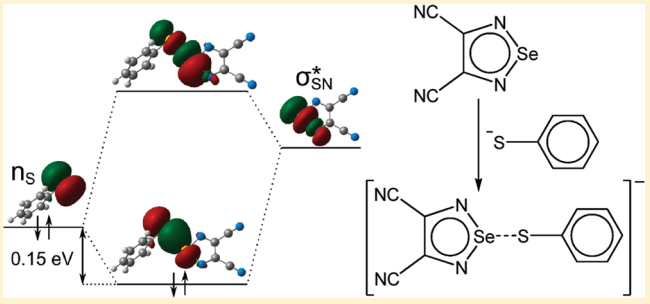

I. INTRODUCTION

The π-delocalized radical anions (π-RAs) play an important role as key intermediates in fundamental organic and main group chemistry.[1] Some of the π-RAs isolated in the form of thermally stable salts have found applications in the field of molecule-based functional materials as charge and/or spin carriers. They are represented mainly by derivatives of cyanocarbons, such as TCNE and TCNQ, (semi)quinones, and nitrogen heterocycles, such as azines.[2−7]

Interesting prospects of further progress are associated with chalcogen—nitrogen chemistry[8−10] with special emphasis on heavier chalcogens.[10,11] Many chalcogen—nitrogen π-heterocycles, for example, derivatives of the 6π-electron 1,2,5-chalcogenadiazole ring system (**1**, Chart 1) forming numerous family of compounds,[9] possess positive electron affinity (EA) meaning that their π-RAs are thermodynamically more stable than neutral molecules.[12] Among them, the π-RAs of 2,1,3-benzothiadiazole (**2**), its Se congener (**3**), and [1,2,5]thiadiazolo[3,4-*c*][1,2,5]thiadiazole (**4**) (Chart 1) have been known since the 1960s as products of reduction of the corresponding heterocycles with alkali metals.[13] However, under those conditions only π-RA salt [K(THF)][**2**] has been isolated.[14]

Recently, new methods for preparation and isolation of the chalcogen—nitrogen π-heterocyclic RAs were suggested based in particular on reduction of neutral precursors with sandwich organometallics,[15] tetrakis(dimethylamino)ethene (TDAE),[16] and chalcogenolates PhX^- (X = S, Se).[17] These methods allowed us to obtain a number of crystalline salts of the π-RAs of **4** and its Se congener (**5**, Chart 1) followed by experimental and theoretical investigation of their magnetic properties. In all cases, except $[TDAE]^{2+}[\mathbf{4}]_2^-$ featuring diamagnetic π-dimers of the RAs,

Received: March 1, 2011
Revised: April 4, 2011
Published: April 18, 2011

Chart 1

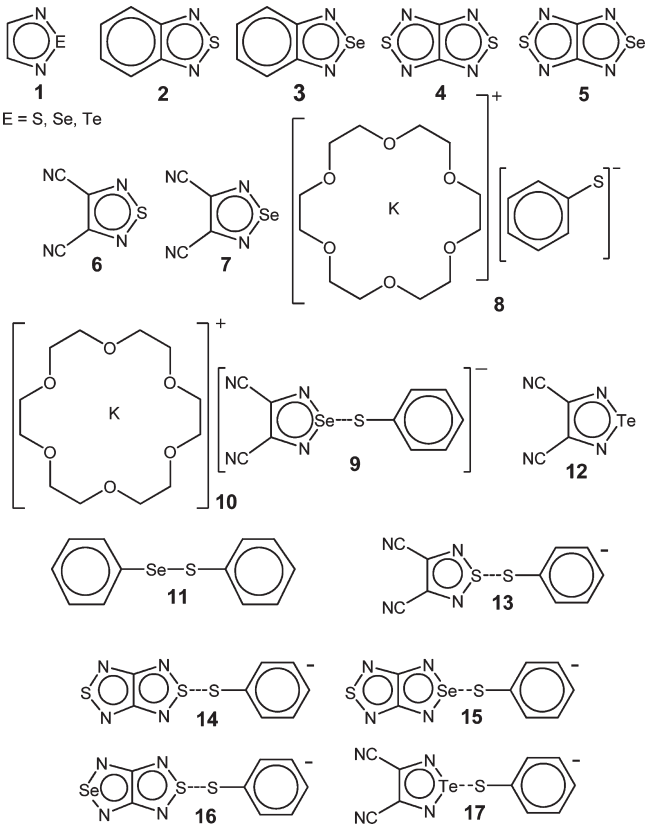

magnetic exchange interactions in spin systems of the salts were observed and explained.[15−17]

The main synthetic target of further research of chalcogen−nitrogen π-RAs is preparation of their heterospin salts with paramagnetic metal cations. In principle, it can be achieved with ArX^-chalcogenolates of d and f metals[18] as reducing agents, sources of required cations.

In this work, the reactivity of 3,4-dicyano-1,2,5-thiadiazole and its Se congener (**6** and **7**, respectively; Chart 1), having nearly the same EA as **4** and **5** according to the DFT calculations, toward PhS^- was studied. Under the CV conditions **6** and **7**, similar to **2**−**5**, readily produced long-lived π-RAs characterized by EPR. However, **6** did not react with $[K(18\text{-crown-}6)]^+[PhS]^-$ (**8**), whereas **7** formed the product of hypercoordination at the Se center (**9**) isolated in the form of the thermally stable salt [K(18-crown-6)][**9**] (**10**) characterized by X-ray diffraction (XRD). The latter type of reactivity has never been observed previously for any 1,2,5-chalcogenadiazole derivatives.[9] In the context of interchalcogen interactions,[11] salt **10** also provides a new example.

To estimate the scope of the observed new reaction, the thermodynamics and kinetics of the interaction between PhS^- and various 1,2,5-chalcogenadiazoles (chalcogen = S, Se, Te) were theoretically investigated within the interchalcogen hypercoordination vs reduction to π-RA dichotomy. The electronic structure of the products of hypercoordination of the PhS^- at the chalcogen centers and the nature of the interchalcogen bonding were studied using DFT calculations, the quantum theory of atom in molecule (QTAIM), and the concept of the natural bond orbitals (NBO).

EXPERIMENTAL AND COMPUTATIONAL DETAILS

General Procedures. Solvents were distilled under argon with common drying agents. ^1H, ^{13}C, ^{14}N, and ^{77}Se NMR spectra (Supporting Information Table S1) were measured with a Bruker DRX-500 instrument at frequencies of 500.13, 125.76, 36.13, and 95.38 MHz with standards TMS (^1H, ^{13}C), NH_3 (liq.) (^{14}N) and Me_2Se (^{77}Se). UV−vis (Table S1, Supporting Information) and IR spectra were recorded on Hewlett-Packard 8453 and Bruker Vector 22 instruments, respectively. Solutions of the salt **10** for UV−vis measurements were prepared under argon using a glovebox.

Syntheses. Compounds **6** and **7** (Tables S1 and S2 and Figures S1 and S2, Supporting Information) were prepared by known methods[19] and purified by vacuum sublimation followed by crystallization from hexane; **6**, mp 53−54 °C; **7**, mp 98−99 °C.

Compound **8** was synthesized as described before.[17b] Crystals suitable to XRD (Table S2, Supporting Information) were obtained by crystallization from a two-layer THF/pentane system under conditions of solvents diffusion at ambient temperature.

Compound 10. Schlenk and glovebox techniques were used. At −30 °C and under argon, to a stirred solution of 0.412 g (0.001 mol) of **8** in 10 mL of THF a solution of 0.183 g (0.001 mol) of **7** in 5 mL of THF was added dropwise. The cherry-red reaction mixture was warmed up to ambient temperature for 30 min and then filtered. Under vacuum, 15 mL of pentane was recondensed onto the filtrate at −196 °C and the two-layer system obtained kept at ambient temperature until mutual diffusion of solvents ceased. Under argon, the solvents were removed with a syringe and the crystalline residue was washed with Et_2O and dried under vacuum. The salt **10** (Tables S1 and S2 and Figure S4, Supporting Information) was obtained as transparent ruby prisms: yield 0.583 g (98%), mp 87 °C (decomp.). Anal. Calcd for $C_{22}H_{29}KN_4O_6SSe$: C, 44.36; H, 4.91; N, 9.41; S, 5.38. Found: C, 44.62; H, 4.93; N, 9.52; S, 5.57.

Cyclic Voltammetry. The CV measurements (Figure S3, Supporting Information) on degassed 2×10^{-3} M solutions of compounds **6** and **7** in MeCN were performed at 295 K in an argon atmosphere using the equipment described previously.[12b] The measurements were carried out in a mode of triangular pulse potential sweep in a three-electrode electrochemical cell ($V = 5$ cm^3) at a stationary platinum electrode ($S = 8$ mm^2), with 0.1 M Et_4NClO_4 as a supporting electrolyte. The sweep rates were 0.01−10 V·s^{-1}; the peak potentials were quoted with reference to a saturated calomel electrode. Electrochemical generation of RAs for EPR measurements was performed at 295 K with 10^{-3} M solutions in MeCN with the same supporting electrolyte in a standard cell for variable-temperature EPR measurements under anaerobic conditions equipped with a stationary platinum electrode at corresponding E_p^{1C} potentials (Figure S3, Supporting Information).

EPR Measurements. EPR spectra were recorded on a Bruker ESP-300 spectrometer (MW power of 265 mW, modulation frequency of 100 kHz, and modulation amplitude of 0.005 mT) equipped with a rectangular double resonator. Numerical simulations of the experimental EPR spectra were performed with the Winsim 2002 program[20] using the Simplex algorithm for optimization of hyperfine coupling constant (hfc) values and line widths. The accuracy in hfc calculation was ±0.001 mT. The half-life times ($\tau_{1/2}$) of RAs were calculated from the time dependence of the double-integral intensities of EPR signals in the absence of an applied potential using the first-order kinetic

dx.doi.org/10.1021/jp2019523 |J. Phys. Chem. A 2011, 115, 4851–4860

equation for the RAs decay ($I = Ae^{(-kt)} + B$, $\tau_{1/2} = 0.69\ k^{-1}$). The g values of RAs were measured with Mn^{2+} in blende with an accuracy of ±0.0002.

Crystallographic Analysis. The XRD data (Table S2, Supporting Information) for **6**, **7**, and **10** were collected on a Bruker APEX-II CCD diffractometer using φ, ω scans of narrow (0.5°) frames and for **8** on a Siemens P4 diffractometer using $2\theta/\omega$ scans with Mo Kα radiation (λ = 0.71073 Å) and a graphite monochromator. The structures were solved by direct methods and refined by full-matrix least-squares method against all F^2 in anisotropic approximation using the SHELX-97 programs set.[21] For **10**, the H-atom positions were calculated with the riding model. Absorption corrections were applied empirically using SADABS programs.[21] The obtained crystal structures were analyzed for short contacts between nonbonded atoms using the PLATON program.[22]

Crystal Structure Data for 8. $C_{18}H_{29}KO_6S$, M = 412.57, monoclinic, a = 12.864(1) Å, b = 18.999(2) Å, c = 8.785(1) Å, β = 102.25(1)°, V = 2098.2(4) Å^3, space group Cc, Z = 4, D_c = 1.306 g.cm^{-1}, μ(Mo Kα) = 0.382 mm^{-1}, $F(000)$ = 880, crystal size 0.90 × 0.70 × 0.70 mm, $2\theta_{max}$ = 27.5°, 9318 reflections collected, 4747 unique reflections (R_{int} = 0.0321) measured, 238 parameters, $R1$ [$I > 2\sigma(I)$] = 0.0329, $wR2$ = 0.0854, S = 1.057 for all data, residual electron density peaks of +0.47 and −0.29 e·Å^{-3}.

Crystal Structure Data for 10. $C_{22}H_{29}KN_4O_6SSe$, M = 595.61, monoclinic, a = 12.4946(4) Å, b = 12.9907(4) Å, c = 16.6219(6) Å, β = 96.950(2)°, V = 2678.14(15) Å^3, space group $P2_1/n$, Z = 4, D_c = 1.477 g·cm^{-1}, μ(Mo Kα) = 1.678 mm^{-1}, $F(000)$ = 1224, crystal size 0.58 × 0.20 × 0.15 mm, $2\theta_{max}$ = 35.0°, 68 600 reflections collected, 11 786 unique reflections (R_{int} = 0.0576) measured, 316 parameters, $R1$ [$I > 2\sigma(I)$] = 0.0259, $wR2$ = 0.0627, S = 1.052 for all data, residual electron density peaks of +0.62 and −0.29 e·Å^{-3}.

Tables listing detailed crystallographic data, atomic positional parameters, and bond lengths and angles are available as CCDC-805246 (**6**), CCDC-805247 (**7**), CCDC-805366 (**8**), and CCDC-805248 (**10**) from the Cambridge Crystallographic Data Centre.

Quantum Chemical Calculations. The (U)B3LYP/6-31+G(d)[23] method was used since it was successfully employed earlier for calculating properties of various closed- and open-shell chalcogen−nitrogen rings and cages including π-RAs[12b,14,15,17,24] and for modeling nucleophilic attack at selenium in diselenides and selenosulfides.[11f] The M06-2X[25] and B97-D[26] functionals were also employed in calculations of the S−E bond energies (E = S, Se, Te) and reaction free energies. The Def2SVP basis set with ECP was employed for Te.[27] The UV−vis spectra were calculated by time-dependent DFT[28] with the M06-HF functional.[29] All calculations were performed with the GAUSSIAN09 suite of programs.[30] Calculations for the THF and MeCN solutions were carried out with the polarizable continuum model (IEFPCM)[31] with radii and nonelectrostatic terms of Truhlar and co-workers' SMD solvation model[32] as implemented into the GAUSSIAN09 suite of programs.[30] QTAIM calculations were performed with the AIMAll program.[33]

RESULTS AND DISCUSSION

The first adiabatic EAs of **6** and **7** calculated at the (U)B3LYP/6-31+G(d) level of theory are 1.84 and 1.94 eV, respectively, as compared with 2.14 and 2.19 eV for **4** and **5** and 0.95 and 1.06 eV for **2** and **3**, respectively. In MeCN as solvent, compounds **6** and **7** (Supporting Information, Table S1 and Figures S1 and S2) were electrochemically reduced into their π-RAs at potentials of −1.07 and −1.03 V, respectively (Figure S3, Supporting Information); the reduction was one-electron, reversible and diffusion controlled. The corresponding potentials of **2**, **3**, **4**, and **5** are −1.51, −1.40, −0.59, and −0.53 eV, respectively.[1f,17a,17c] The π-RAs were long-lived with $\tau_{1/2}$ (295 K) of 125 and 500 s in the case of **6** and **7**, respectively. The π-RAs were identified by EPR (Figure 1), and the agreement between experimental and DFT-calculated hfc constants was good.

Previously, thiolate salt **8** (Figure 2a, Table S2, Supporting Information) was used for reduction of **4** and **5** into their π-RAs (Scheme 1); on the other hand, **8** did not reduce **2** and **3**.[17] With **6** and **7** it was found that PhS^- does not interact with **6**, whereas in the case of **7** hypercoordination of PhS^- to the Se center was observed to give anion **9** isolated in the form of salt **10** (Scheme 1). The structure of salt **10** was confirmed by XRD (Figure 2b; Table S2 and Figure S4, Supporting Information). Formation of salt **10** is the first example of nucleophilic hypercoordination to the chalcogen center of 1,2,5-chalcogenadiazole derivatives for which interactions with electrophilic reagents at the N centers are typical.[9,34]

Salt **10** is EPR silent in the solid state and solutions in THF and MeCN. Its solutions have a cherry-red color (Figure 3a, Table S1, Supporting Information), whereas solutions of **7** and **8** are colorless (Table S1, Supporting Information). The ^{77}Se NMR signal of **10** is shifted downfield by ca. 45 ppm as compared with that of **7** (Table S1, Supporting Information). The crystalline salt is stable toward atmospheric moisture and oxygen which is different from the properties of previously studied 1,2,5-thiadiazolidyl salts.[14,17,35] In THF solution, however, **10** slowly decomposes; visible light facilitates decomposition.

The most interesting structural feature of anion **9** is the Se−S distance of 2.722 Å, which is ca. 0.5 Å longer than the sum of the covalent radii of these atoms of 2.25 Å[36] but ca. 1 Å shorter than the sum of their vdW radii.[37] For derivatives of Ph−Se−S−Ph (**11**) with known XRD structures the Se−S bond length varies in the range 2.20−2.22 Å,[38] for neutral derivatives of 3-coordinated Se atom in the range 2.50−2.58 Å,[39] and for derivatives of the 4-coordinated Se atom in the range 2.78−3.05 Å.[40] The Se−S bond of **9** will be discussed in detail below.

The structure of anion **9** as well as of the ion pair [K(18-crown-6)][**9**] was optimized at the B3LYP/6-31+G(d) level of theory. Comparison of the calculated structure of **9** (Figure S5, Supporting Information) with the experimental one (Figure 2b) demonstrates fairly good agreement, particularly, the optimized Se−S bond distance of 2.705 Å is very close to the experimental one of 2.722 Å. The calculated IR spectrum of the ion pair [K(18-crown-6)][**9**] reproduces very well the experimental IR spectrum of the salt **10** (Figure S6, Supporting Information). The Se−S stretching vibration of **9** contributes mainly to the IR band at 165 cm^{-1} (Figure S6, Supporting Information), i.e., at expectedly lower frequency as compared with the S−S stretching vibrations in, for example, aromatic disulfides (430−510 cm^{-1}).[41]

Calculations of the UV−vis spectrum of anion **9** as well as that of ion-pair [K(18-crown-6)][**9**] were performed within the PCM model using time-dependent DFT with the specially proposed M06-HF functional[29] because it is well known that TD-DFT calculations with conventional functionals (e.g., B3LYP) significantly underestimate the excitation energies for the CT excited

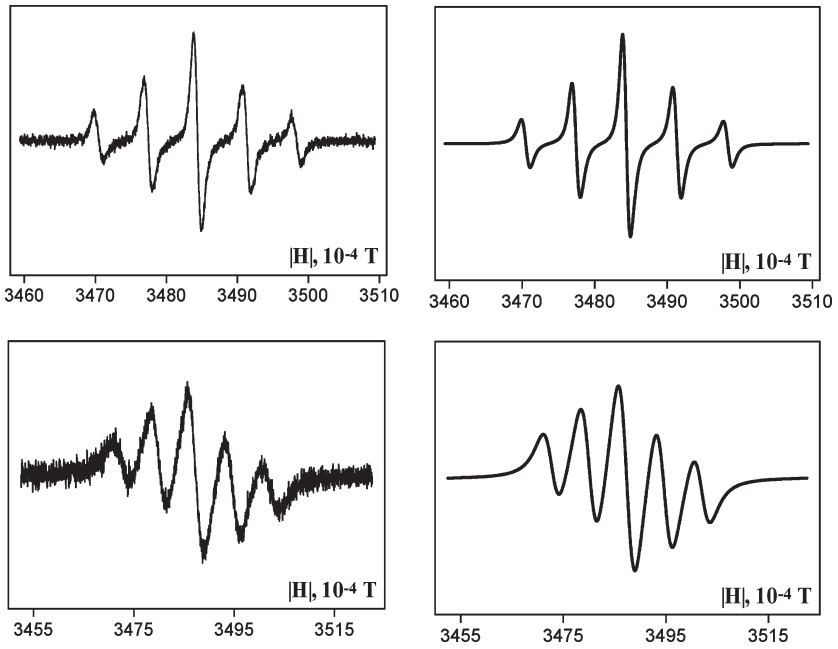

Figure 1. Experimental (left) and simulated (right) EPR spectra of π-RAs of **6** (top) and **7** (bottom) in MeCN. Experimental (calculated at the UB3LYP/6-31+G(d) level) hfs constatnts $a(^{14}N_{cycle} \times 2)$ and $a(^{14}N_{CN} \times 2)$ (mT): **6** 0.698 (0.741), 0.023 (0.034); 7 0.730 (0.762), not resolved (0.032). *g* Values: **6**, 2.00191; **7**, 2.00025.

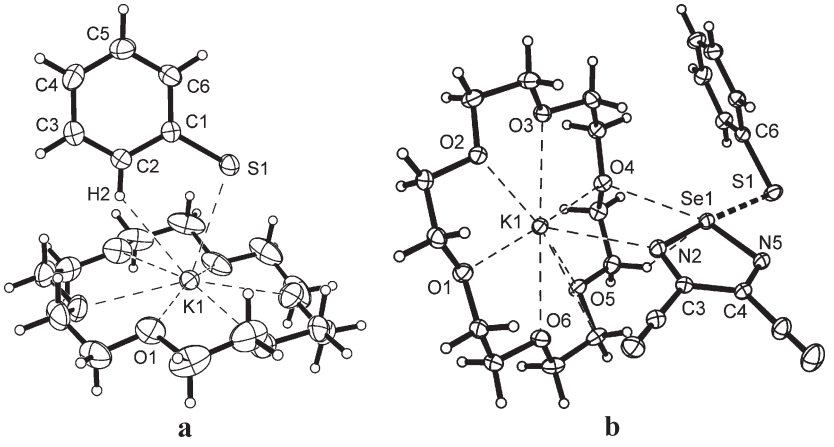

Figure 2. XRD structure of **8** (a) and **10** (b). Selected bond distances (Å) and bond angles (deg): **8**: C1−S1 1.747(2), S1···K1 3.1130(7); C1−S1···K1 101.66(7). **10**: Se1−S1 2.7217(3), Se1−N5 1.8126(8), Se1−N2 1.8734(9), S1−C6 1.755(1), N2−C3 1.303(1), C3−C4 1.438(1), C4−N5 1.310(1), N5−Se1−N2 90.27(4), S1−Se1−N2 175.15(3), S1−Se1−N5 87.44(3), K···O 2.7615(8)−2.8315(8).

states.[28] Figure 3a demonstrates that the position of the lowest energy transition calculated at the M06-HF/6-31G(d) level coincides well with the maximum of the experimental long-wavelength band (e.g., 421 and 451 nm in MeCN). According to the calculations, this band can be assigned mainly to the HOMO → LUMO excitation. Since these MOs have different spatial localization (Figure 3b), the excitation is accompanied by the charge transfer from the phenylthio fragment onto the heterocyclic part of **9**. Thus, this band can be considered as a charge-transfer (CT) band. As expected,[28] the TD-B3LYP calculations underestimate significantly the energy of this transition (631 nm).

One can conclude that the DFT calculations reproduce well the geometry and spectroscopic properties of hypercoordinate anion **9** with its relatively long Se−S bond. The energy of the Se−S bond in **9** was calculated as a difference in the electronic energies of the separated species (PhS^- and **7**) and anion **9** in the gas phase (Table 1). Since it is known that conventional DFT functionals such as B3LYP perform unreliably for the description of weakly bonded complexes (e.g., donor−acceptor, van der Waals, and H-bonded complexes),[25,26,29,42] two new functionals taking into account long-range dispersion interactions,[42] namely, M06-2X[25] and B97-D,[26] were also employed. For generality, putative ions **13**−**17** (Chart 1) were also calculated (Table 1) including that derived from recently described tellurium−nitrogen heterocycle **12**[43] whose calculated first adiabatic EA of 2.04 eV is comparable with those of **6** and **7**. The gas-phase structures of anions **13**−**17** were optimized using three aforementioned DFT procedures, and all structures were ascertained to be minima on the potential energy surfaces.

Scheme 1

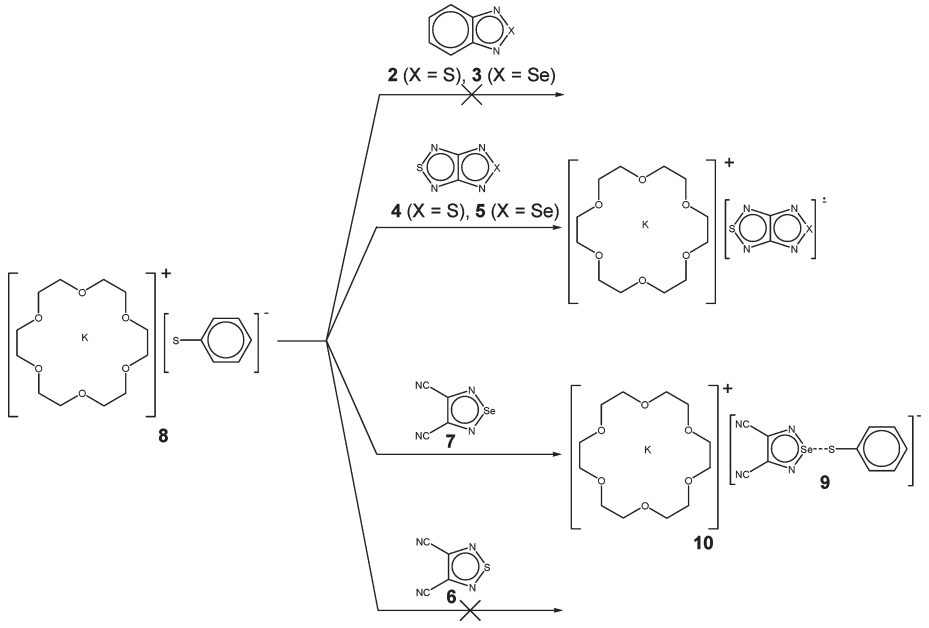

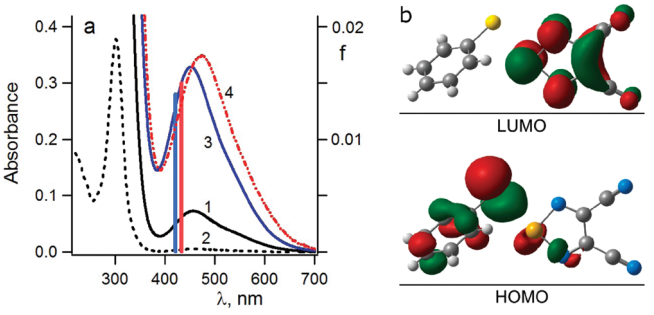

Figure 3. (a) Experimental UV−vis spectra of **10** (1.38×10^{-4} M) in MeCN in 10 (1) and 1 mm (2) cuvettes and in MeCN (3) and THF (4) solutions of **10** and **7** ([**10**] = 1.38×10^{-4} M, [**7**] = 2.8×10^{-2} M, l = 10 mm for spectrum 3; [**10**] = 3.05×10^{-4} M, [**7**] = 2.5×10^{-2} M, l = 5 mm for spectrum 4). As **9** is in equilibrium with PhS^- and **7** (see below), the excess of heterocycle **7** was added. The vertical bars indicate the positions and oscillator strengths (f, right axis) of the long-wavelength electronic transitions calculated at the M06-HF/6-31G(d) level for the ion pair [K(18-crown-6)][**9**] in MeCN (blue bar) and THF (red bar). (b) HOMO and LUMO of **9** calculated at the same level of theory.

At the B3LYP level, the calculated energy of the Se−S bond in **9** (28.9 kcal/mol) is much lower than that of selenosulfide **11** (37.1 kcal/mol). At the M06-2X and B97-D levels, the energy of the Se−S bond in **9** is predicted to be noticeably higher (Table 1).

Table 1 demonstrates that DFT calculations predict similar interchalcogen bond lengths in the gas-phase structures of all considered anions (2.58−2.89 Å depending to a great extent on the level of theory employed). According to the calculations the Se−S bonding in anion **9** is noticeably stronger than the S−S bonding in the putative anions **13**, **14**, and **16** (E_{bond}^{BSSE} is higher by about 3−10 kcal/mol depending on the anion and level of theory, Table 1). As expected, the calculations predict a significantly stronger Te−S bond in anion **17** (E_{bond}^{BSSE} is higher by about 10−15 kcal/mol) than the Se−S bond in **9**.

To get deeper insight into the characteristics of the interchalcogen bonding in **9**, QTAIM[44] and NBO[45] analyses were carried out for the optimized structure of this anion. Recently, these techniques were successfully used for the in-depth investigation of various Se···X secondary bonding interactions.[11,46] The first evidence of the bonding according to the QTAIM approach is the existence of a bond path between two atoms and of a bond critical point (BCP) in the middle of the path.[44] The QTAIM calculations identified the BCP for the Se−S bond of **9** shifted slightly to the Se atom and featuring a value of ca. 0.05 for both ρ_{BCP} and $\nabla^2\rho_{BCP}$ as compared with ca. 0.11 and −0.04, respectively, for analogues BCP in **11** (Figure 4; ρ and $\nabla^2\rho_{BCP}$ are the electronic density and its Laplacian, respectively, in au). Note that negative values of $\nabla^2\rho_{BCP}$ are typical of the covalent bonds.[44] In turn, the positive values of Laplacian in BCP are typical of the closed-shell interactions (e.g., donor−acceptor and hydrogen bonding).[44]

NBO analysis[45] allows one to describe formation of the Se−S bond of **9** as an interaction of the lone pair localized at the S atom of the PhS^- anion with the σ^*-antibonding orbital of the Se−N bond of heterocycle **7** (Figure 5). The interaction requires a face-to-edge orientation of molecular planes of reaction partners and exactly this orientation featuring the DFT-optimized structure of **9** (Figure S5, Supporting Information) as well as the experimental one (Figure 2b).

Therefore, results of the QTAIM and NBO analysis indicate that the Se−S bond in **9** came from interaction of closed-shell species and can be classified as a donor−acceptor bond. The QTAIM-calculated atomic charges (Figure 4) suggest a significant contribution from the Coulombic interaction between oppositely charged Se and S atoms into formation of the Se−S bond of **9**. The same also follows from the charge distribution calculated with the Merz−Kollman approach[47] despite it giving different effective charges for Se and S. Both distributions reveal that ca. 38% of the negative charge is transferred from PhS^- onto the heterocycle upon Se−S bond formation (Figure 4).

dx.doi.org/10.1021/jp2019523 |J. Phys. Chem. A 2011, 115, 4851–4860

Table 1. Calculated Interchalcogen Bond Lengths (r) and Energies (E_{bond}) of Hypercoordinate Anions[a]

	r, Å			E_{bond}, kcal/mol			E_{bond}^{BSSE}, kcal/mol		
anion	B3LYP	B97-D	M06-2X	B3LYP	B97-D	M06-2X	B3LYP	B97-D	M06-2X
9	2.70	2.73	2.68	28.9	35.9	37.6	23.8	30.9	32.6
13	2.79	2.82	2.79	21.1	23.6	25.6	20.5	23.0	25.0
14	2.82	2.89	2.61	19.2	21.9	23.8	18.5	21.0	23.0
15	2.85	2.87	2.58	22.4	31.4	32.1	16.7	24.8	26.4
16	2.75	2.83	2.58	19.5	24.3	24.6	17.8	22.4	23.0
17	2.75	2.78	2.70	39.0	43.5	43.6	38.3	42.9	42.9

[a] All calculations were performed for the gas phase with a 6-31+G(d) basis set for all atoms except Te, for which the Def2SVP basis set with ECP was employed; BSSE was taken into account in the E_{bond}^{BSSE} values.

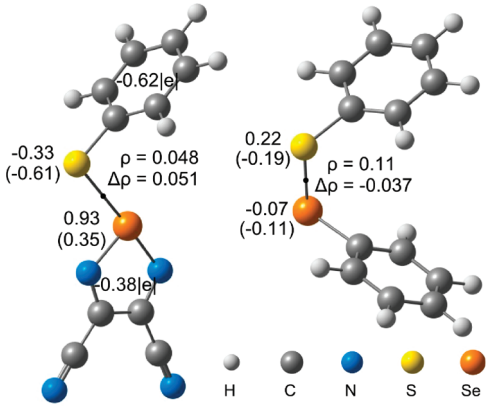

Figure 4. BCPs of the Se−S bonds and QTAIM charge distributions in **11** (right) and **9** (left) together with the Merz−Kollman charges on chalcogen atoms (in parentheses).

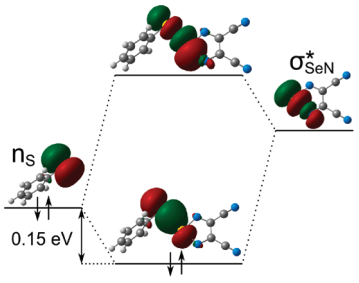

Figure 5. NBO diagram for Se−S bond formation in **9**.

To estimate the thermodynamics of the reactions between thiophenolate and heterocycles **4**−**7** and **12**, the free energies of hypercoordination were calculated in two solvents, THF and MeCN, using the PCM model (Table 2). In THF and MeCN solutions, formation of products of hypercoordination is predicted to be thermodynamically attractive for heterocycles **7** and **5** with formation of the Se−S bond and for **12** with formation of the Te−S bond. The hypercoordination of PhS^- with formation of the S−S bond (**13**, **14**, and **16**) is predicted to be endothermal or close to thermoneutral (Table 2). Although formation of **9** is predicted to be exothermal (Scheme 1), the enthalpy of reaction is low (Table 2) and anion **9** should be in the equilibrium with reagents PhS^- and **7**.

Spectroscopic measurements revealed that the effective extinction coefficient (ε_{eff}) of the salt **10** CT band (Figure 3a) depends strongly on the solution concentration, namely, the value of ε_{eff} decays significantly with the decrease of concentration. On the contrary, addition of **7** (having no absorption in the visible region, Table S2, Supporting Information) to the MeCN solution of **10** leads to pronounced growth of the long-wavelength absorption (Figure 3a); adding **7** to the THF solution of **10** results in the less pronounced growth of absorption. These observations indicate that in solution anion **9** is indeed in the equilibrium with PhS^- and **7**, and in MeCN in the range of concentrations employed ($<10^{-3}$ M) the equilibrium is shifted to the dissociated state.

Table 2. Calculated Free Energy of Reactions (ΔG_{react}^{calcd}) at 298 K in THF and MeCN (in parentheses)[a,b]

	ΔG_{react}^{calcd}, kcal/mol		
reaction	B3LYP	M06-2X	B97-D
7 + PhS^- → **9**	−0.8 (1.1)	−3.5 (−1.8)	−7.2 (−3.6)
6 + PhS^- → **13**	5.1 (6.2)	2.2 (3.9)	1.7 (3.8)
4 + PhS^- → **14**	3.7 (3.8)	1.8 (2.8)	−1.2 (−0.5)
5 + PhS^- → **15**	−3.9 (−1.9)	−6.1 (−4.6)	−7.3 (−5.6)
5 + PhS^- → **16**	4.0 (5.4)	1.1 (3.1)	0.01 (−1.8)
12 + PhS^- → **17**	−4.3 (−0.3)	−7.0 (−3.2)	−9.1 (−5.5)

[a] All calculations were performed with the 6-31+G(d) basis set for all atoms except Te, for which the Def2SVP basis set with ECP was employed. [b] Experimental values of the equilibrium constant (K) and free energy (ΔG_{react}^{exp}) of the reaction between **7** and PhS^- in THF and MeCN (in parentheses): $K = 7.4 \pm 1.0 \times 10^4$ ($3.0 \pm 0.6 \times 10^3$) $l.mol^{-1}$; $\Delta G_{react}^{exp} = -6.6 \pm 0.1$ (-4.7 ± 0.1) kcal/mol.

UV−vis spectroscopy makes it possible to measure equilibrium constants (Figure S7, Supporting Information) and estimate the free energies of this reaction in THF and MeCN (Table 2). Data of Table 2 demonstrate that the reaction free energies calculated with the B97-D functional (−7.2 and −3.6 kcal/mol) are in very good agreement (within 1 kcal/mol) with experiment (−6.6 ± 0.1 and −4.7 ± 0.1 kcal/mol). Thus, taking into account long-range dispersion interactions is important for accurate predictions of the properties of the discussed hypercoordinate products.

To rationalize the hypercoordination vs reduction dichotomy observed, the thermodynamics and kinetics of the electron transfer (ET) from PhS^- onto **2**, **4**−**7**, and **12** were theoretically studied (Table 3). It was found that the B3LYP-calculated free energy of the ET reaction in MeCN correlates linearly with the first reduction peaks (E_p^{1C}) of **2** and **4**−**7** (Figure S8, Supporting Information). The slope is close to unity (1.16 ± 0.11), which indicates that the B3LYP functional is appropriate for the analysis of the ET reaction under consideration.

dx.doi.org/10.1021/jp2019523 |J. Phys. Chem. A 2011, 115, 4851–4860

Table 3. Calculated Free Energies of the ET Reaction (ΔG_{calcd}°) in MeCN and THF, Experimental Potentials of One-Electron Reduction in MeCN (E_p^{1C}), Solvent (λ_s) and Intramolecular (λ_{in}) Reorganization Energies, and Theoretically Estimated Rate Constants of the ET Reaction (k) in THF[a]

	ΔG_{calcd}° kcal/mol					
reaction	MeCN	THF	E_p^{1C}, V	λ_s, kcal/mol	λ_{in}, kcal/mol	k, M^{-1} s^{-1}
$PhS^- + 7 \rightarrow PhS^{\bullet} + 7^-$	31.7	28.9	−1.03	15.2	5.5	9×10^{-11}
$PhS^- + 6 \rightarrow PhS^{\bullet} + 6^-$	28.9	26.9	−1.07	15.3	5.9	5×10^{-9}
$PhS^- + 5 \rightarrow PhS^{\bullet} + 5^-$	17.3	15.8	−0.53	15.5	4.2	1
$PhS^- + 4 \rightarrow PhS^{\bullet} + 4^-$	14.3	13.4	−0.59	15.2	4.7	25
$PhS^- + 2 \rightarrow PhS^{\bullet} + 2^-$	40.8	40.3	−1.51	15.0	4.6	2×10^{-22}
$PhS^- + 12 \rightarrow PhS^{\bullet} + 12^-$	30.5	27.6		14.4	4.8	7×10^{-10}

[a] All calculations were performed at the B3LYP/6-31+G(d) level of theory (for Te the Def2SVP basis set with ECP was employed).

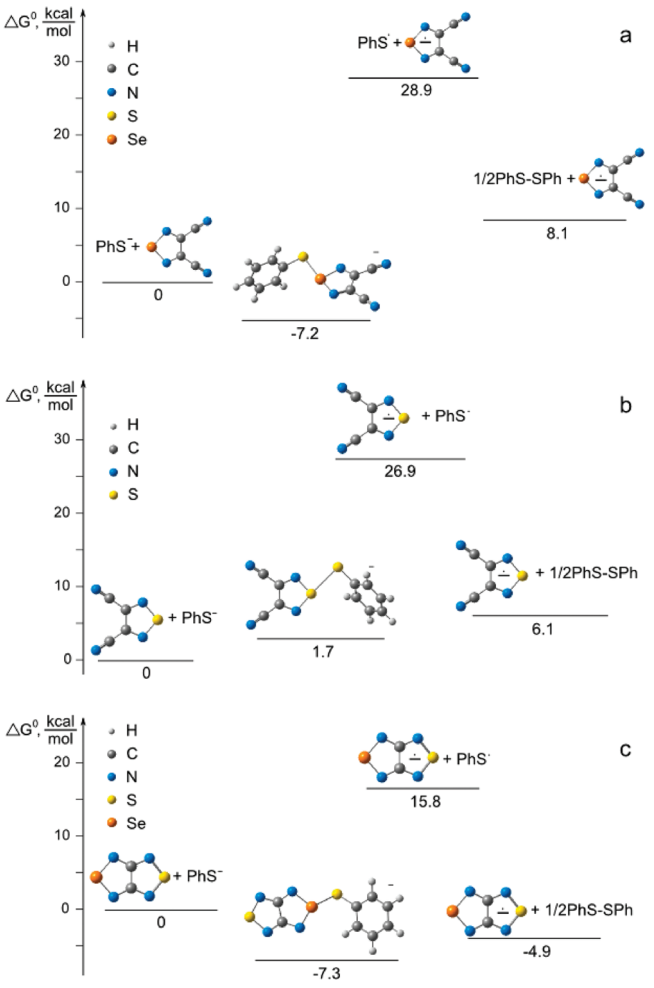

Figure 6. Free energy diagrams for the reactions of PhS^- with **7** (a), **6** (b), and **5** (c) in THF. The values of ΔG° for the ET pathway were calculated at the B3LYP level and those for the hypercoordination one at the B97-D level.

The rate constants of the ET reactions (k) have been estimated in the framework of the Marcus approach[48] using formula 1 under the assumption that the reactions are adiabatic, notably, the pre-exponent A is equal to 3×10^{11} M^{-1} s^{-1}. In the formula 1, k_B is the Boltzmann constant, ΔG° is the free energy of the ET reaction, and λ is the reorganization energy. λ is the sum of two components: the solvent reorganization energy (λ_s) and the reorganization energy of the donor and acceptor (λ_{in})

$$k = A \times \exp\left[\frac{-(\Delta G^{\circ} + \lambda)^2}{4\lambda k_B T}\right] \quad (1)$$

Values of λ_s (Table 3) were estimated using a simple formula, eq 2, where ε_s and ε_{op} are static and optical (square of refractive index) dielectric constants of the solvent, respectively.[48] The effective radii of the molecule and anion (a_1, a_2) were obtained from the DFT calculations. Values of λ_{in} (Table 3) were calculated at the B3LYP level

$$\lambda_s = e^2\left(\frac{1}{2a_1} + \frac{1}{2a_2} - \frac{1}{r}\right)\left(\frac{1}{\varepsilon_{op}} - \frac{1}{\varepsilon_s}\right) \quad (2)$$

For **2**, **6**, **7**, and **12**, negligible k values (Table 3) practically exclude this reaction proceeding under normal conditions (for nonadiabatic reactions the k values should be even smaller). On the contrary, for **4** and **5** calculated k values suggest relatively fast reactions, which is in agreement with the observation that in these cases π-RAs form immediately upon mixing reagents at −30 °C.[17]

It is clear that the ET is reversible and the equilibrium is shifted to the reagents. However, one of the products, radical $PhS^{\bullet}$, undergoes recombination to PhS−SPh. Figure 6 displays three situations which can be realized in the reaction of PhS^- with discussed 1,2,5-chalcogenadiazole derivatives. In the reaction with **7** (Figure 6a) the product of hypercoordination is thermodynamically most favorable, the ET rate constant is very low (Table 3), and, namely, in this case anion **9** was isolated. PhS^- does not react with **6** (Figure 6b) as the reagents are thermodynamically preferable. For **5** the ET is fast on the time scale of the chemical experiment (Table 3) and formation of such final products as corresponding π-RAs and PhS−SPh is thermodynamically favorable (Figure 6c). The same is also true for **4**.

In the case of **12**, Te congener of **7**, the B97-D free energy of the hypercoordinate anion formation in THF is −9.1 kcal/mol. Similar to the case of **7**, the ET from PhS^- onto **12** was predicted to be unfavorable with ΔG° = 27.6 kcal/mol and $k \approx 6 \times 10^{-9}$ M^{-1} s^{-1}. Thus, the hypercoordinate product **17** is expected to be isolated in this case. Corresponding experiments are in progress.

CONCLUSIONS

Experimental and theoretical results obtained in this work extend the scope of the interchalcogen interactions with special emphasis on the heavier chalcogens. We succeeded to observe

dx.doi.org/10.1021/jp2019523 |J. Phys. Chem. A 2011, 115, 4851–4860

experimentally the first example of nucleophilic hypercoordination of the thiophenolate at the Se center of the 1,2,5-chalcogenadiazole derivative, compound **7**. The XRD structure of the hypercoordinate product, anion **9**, revealed the elongated Se−S bond distance of ca. 2.7 Å. This interchalcogen bond can be considered as a weak donor−acceptor bond whose formation is accompanied by transfer of ca. 38% of negative charge from the exocyclic part of the anion onto the heterocyclic part. Coulombic interaction between oppositely charged Se and S atoms also contributes to interchalcogen bonding in **9**.

The influence of the nature of the chalcogen in the 1,2,5-chalcogenadiazoles on the thermodynamics of the discovered reaction was analyzed computationally. Calculations predict that hypercoordination of PhS^- with formation of the S−S bond is almost thermoneutral. In accordance with experiment, the hypercoordinate products with the Se−S bond are thermodynamically more preferable. In turn, interaction of PhS^- with the Te congener of **7** is predicted to lead to hypercoordinate anion **17** featuring a stronger Te−S bond than the Se−S bond in anion **9**. Therefore, one can expect the general character of the discussed hypercoordination in the case of heavier chalcogens.

Reduction of 1,2,5-chalcogenadiazoles by PhX^- (X = S, Se) is a very convenient preparative approach to their π-RAs, promising building blocks in the design and synthesis of new molecule-based magnets and/or conductors. At the same time, the ET rate constant seems to be rather variable. The results of this work demonstrate that the hypercoordination with formation of the interchalcogen bond vs reduction to π-RA dichotomy, a delicate balance of thermodynamics and kinetics of the reaction system, should be taken into account.

■ ASSOCIATED CONTENT

Supporting Information. Full citation for the Gaussian09 suit of programs (ref 30), XRD molecular structures of **6** and **7**, XRD crystal structures of **6** and **7**, CV of **6** and **7**, XRD crystal structure of **10**, DFT-optimized structure of **9**, experimental and calculated IR spectra of **10**, dependence of the hypercoordinate product formation on the concentration of **7**, correlation of the calculated free energy of the ET reaction with the first reduction potentials of **3**−**7**, multinuclear NMR and UV−vis data for **6**, **7**, and **10**, full crystal and refinement data of **6**, **7**, **8**, and **10**, and optimized geometries and energies of the hypercoordinate anions. This material is available free of charge via the Internet at http://pubs.acs.org.

■ AUTHOR INFORMATION

Corresponding Author

*E-mail: gritsan@kinetics.nsc.ru (N.P.G.); mews@uni-bremen.de (R.M.); zibarev@nioch.nsc.ru (A.V.Z.).

■ ACKNOWLEDGMENT

The authors are grateful to Mr. Peter Brackmann for his participation in the XRD measurements and to the Deutsche Forschungsgemeinschaft (project 436 RUS 113/967/0-1 R), the Russian Foundation for Basic Research (projects 09-03-00361, 10-03-00735, and 10-03-08249), the Presidium of the Russian Academy of Sciences (project 7.17), and the Siberian Branch of the Russian Academy of Sciences (project 105) for financial support of this work. The support of this work by the Siberian Supercomputer Center is also gratefully acknowledged. N.A.S. thanks the Russian Science Support Foundation for a 2010 Postgraduate Scholarship. A.V.L. is grateful to the Russian Academy of Sciences for the Golden Medal with Premium and to the Russian Federal Ministry for Education and Science for the Diploma, both for Graduates 2009. He also appreciates the support from the Russian Federal Agency for Education (project no. 14.740.11.0716) and the Deutscher Akademischer Austausch Dienst−Russian Ministry for Education and Science joint program "Mikhail Lomonosov" (project 2.2.2.3/9031).

■ REFERENCES

(1) (a) Todres, Z. V. *Ion-Radical Organic Chemistry: Principles and Applications*; CRC Press/Taylor & Francis: Boca Raton, 2009. (b) Denning, M. S.; Irwin, M.; M. Golcoechea, M. *Inorg. Chem.* **2008**, *47*, 6118–6120. (c) Gallardo, I.; Guirado, G.; Marquet, J.; Vila, N. *Angew. Chem., Int. Ed.* **2007**, *46*, 1321–1325.(d) Rusakov, A. I.; Mendkovich, A. S.; Gultai, V. P.; Orlov, V. Yu. *Structure and Reactivity of Organic Radical Anions*; Mir Publishers: Moscow, 2005 (in Russian). (e) Todres, Z. V. *Organic Ion Radicals*; CRC Press: Boca Raton, 2002. (f) Boere, R. T.; Roemmele, T. L. *Coord. Chem. Rev.* **2000**, *210*, 369–445.

(2) (a) Saito, G.; Yoshida, Y. *Bull. Chem. Soc. Jpn.* **2007**, *80*, 1–137. (b) Yagubskii, E. B. In *Organic Conductors, Superconductor, and Magnets: From Synthesis to Molecular Electronics*; Ouahab, L., Yagubskii, E., Eds.; Kluwer: Dordrecht, 2004.

(3) (a) Motokawa, N.; Miyasaka, H.; Yamashita, M.; Dunbar, K. R. *Angew. Chem., Int. Ed.* **2008**, *47*, 7760–7763. (b) Yamashida, Y.; Tomura, T. *J. Mater. Chem.* **1998**, *8*, 1933–1944. (c) Tsubata, Y.; Suzuki, T.; Yamashita, Y.; Mikai, T.; Miyashi, T. *Heterocycles* **1992**, *33*, 337–348. (d) Yamashita, Y.; Mikai, T.; Miyashi, T.; Saito, G. *Bull. Chem. Soc. Jpn.* **1988**, *61*, 483–493.

(4) (a) Choua, S.; Djukic, J. P.; Dallery, J.; Bieber, A.; Welter, R.; Gisselbrecht, J. P.; Turek, P.; Ricard, L. *Inorg. Chem.* **2009**, *48*, 149–163. (b) Gloekle, M.; Hueber, K.; Kuemmerer, H. J.; Denninger, G.; Kaim, W. *Inorg. Chem.* **2001**, *40*, 2263–2269. (c) Schwach, M.; Hausen, H. D.; Kaim, W. *Inorg. Chem.* **1999**, *38*, 2242–2243. (d) Bock, H.; John, A.; Naether, C.; Ruppert, K. *Helv. Chim. Acta* **1994**, *77*, 1505–1509.

(5) (a) Miller, J. S. *J. Mater. Chem.* **2010**, *20*, 1846–1857. (b) Her, J. H.; Stephens, P. W.; Ribas-Arino, J.; Novoa, J. J.; Shum, W. W.; Miller, J. S. *Inorg. Chem.* **2009**, *48*, 3296–3307. (c) Miller, J. S. *Polyhedron* **2009**, *28*, 1596–1605. (d) Miller, J. S. *Dalton Trans.* **2006**, 2742–2749. (e) Miller, J. S. *Inorg. Chem.* **2000**, *39*, 4392–4408. (f) Miller, J. S.; Epstein, A. J. *Angew. Chem., Int. Ed.* **1994**, *33*, 385–415. (g) Miller, J. S.; Epstein, A. J.; Reiff, W. M. *Chem. Rev.* **1988**, *88*, 201–220.

(6) (a) Koizumi, K.; Shoji, M.; Ritawaga, Y.; Takeda, R.; Yamanaka, S.; Kawakami, T.; Okumura, M.; Yamaguchi, K. *Polyhedron* **2007**, *26*, 2135–2141. (b) Broderick, W. E.; Eichhorn, D. M.; Liu, X.; Toscano, P. J.; Owens, S. M.; Hoffman, B. M. *J. Am. Chem. Soc.* **1995**, *117*, 3641–3642. (c) Eichhorn, D. M.; Skee, D. C.; Broderick, W. E.; Hoffman, B. M. *Inorg. Chem.* **1993**, *32*, 491–492. (d) Broderick, W. E.; Hoffman, B. M. *J. Am. Chem. Soc.* **1991**, *113*, 6334–6335. (e) Brandon, R. L.; Osiecki, J. H.; Ottenberg, A. *J. Org. Chem.* **1966**, *31*, 1214–1217.

(7) (a) Lu, J. M.; Rosokha, S. V.; Neretin, I. S.; Kochi, J. K. *J. Am. Chem. Soc.* **2006**, *128*, 16708–16719. (b) Bencini, A.; Daul, C. A.; Dei, A.; Mariotti, F.; Lee, H.; Shulz, D. A.; Sorace, L. *Inorg. Chem.* **2001**, *40*, 1582–1590. (c) Shulz, D. A.; Bodnar, S. H.; Vostrikova, K. E.; Kampf, J. W. *Inorg. Chem.* **2000**, *39*, 6091–6093. (d) Pierpoint, C. G.; Lange, C. W. *Prog. Inorg. Chem.* **1994**, *41*, 331–442. (e) Adams, M.; Dei, A.; Rheingold, A. L.; Hendrickson, D. N. *Angew. Chem., Int. Ed.* **1993**, *32*, 880–882. (f) Dei, A.; Gatteschi, D. *Inorg. Chim. Acta* **1992**, *198*−*200*, 813–822.

(8) (a) Chivers, T.; Laitinen, R. S. In *Handbook of Chalcogen Chemistry. New Perspectives in Sulfur, Selenium and Tellurium*; Devillanova, F., Ed.; RSC Press: Cambridge, U.K., 2007. (b) Chivers, T. *A Guide to Chalcogen-Nitrogen Chemistry*; World Scientific: Singapore, 2005.

(9) (a) Koutentis, P. A. *Comprehensive Heterocyclic Chemistry III*; Pergamon Press: Oxford, 2008; Vol. 5. (b) Yamazaki, R. *Comprehensive Heterocyclic Chemistry III*; Pergamon Press: Oxford, 2008; Vol. 6. (c) Koutentis, P. A. *Sci. Synth.* **2004**, *13*, 297–348. (d) Aitken, R. A. *Sci. Synth.* **2004**, *13*, 777–822. (e) Grivas, S. *Curr. Org. Chem.* **2000**, *4*, 707–726.(f) Shinkai, I.; Reider, P. In *Comprehensive Heterocyclic Chemistry II*; Pergamon Press: Oxford, 1996; Vol. 4. (g) Ulrich, H. *Methoden der Organischen Chemie (Houben-Weyl)*; Thieme: Stuttgart, 1994; Vol. E8d. (h) Weinstock, L. M.; Shinkai, I. *Comprehensive Heterocyclic Chemistry I*; Pergamon Press: Oxford, 1984; Vol. 6.

(10) During the two past decades, numerous chalcogen−nitrogen π-heterocyclic neutral radicals and radical cations were isolated and successfully used as building blocks in the design and synthesis of molecular magnets and conductors. Heavier chalcogen derivatives display enhanced conductivity and larger magnetic exchange interactions. Relevant literature is too abundant to be cited completely. For selected recent work, see: (a) Hicks, R. G. In *Stable Radicals: Fundamentals and Applied Aspects of Odd-Electron Compounds*; Hicks, R. G., Ed.; Wiley: New York, 2010; pp 317−380. (b) Clarke, C. S.; Jornet-Somoza, J.; Mota, F.; Novoa, J. J.; Deumal, M. *J. Am. Chem. Soc.* **2010**, *132*, 17817–17830. (c) Lekin, K.; Winter, S. M.; Downie, L. E.; Bao, X.; Tse, J. S.; Desgreniers, S.; Secco, R. A.; Dube, P. A.; Oakley, R. T. *J. Am. Chem. Soc.* **2010**, *132*, 16212–16224. (d) Tse, J. S.; Leitch, A. A.; Yu, X.; Bao, X.; Zhang, S.; Liu, Q.; Jin, C.; Secco, R. A.; Desgreniers, S.; Ohishi, Y; Oakley, R. T. *J. Am. Chem. Soc.* **2010**, *132*, 4876–4886. (e) Cameron, T. S.; Decken, A.; Grein, F.; Knapp, C.; Passmore, J.; Rautiainen, J. M.; Shuvaev, K. V.; Thompson, R. C.; Wood, D. J. *Inorg. Chem.* **2010**, *49*, 7861–7879. (f) Deumal, M.; Rawson, J. M.; Howard, J. A. K.; Copley, R. C. B.; Robb, M. A.; Novoa, J. J. *Chem.—Eur. J.* **2010**, *16*, 2741–2750. (g) Mito, M.; Komorida, Y.; Tsuruda, H.; Tse, J. S.; Desgreniers, S.; Ohishi, Y.; Leitch, A. A.; Cvrkalj, K.; Robertson, C. M.; Oakley, R. T. *J. Am. Chem. Soc.* **2009**, *131*, 16012–16013. (h) Leitch, A. A.; Yu., X.; Winter, S. M.; Secco, R. A.; Dube, P. A.; Oakley, R. T. *J. Am. Chem. Soc.* **2009**, *131*, 7112–7125. (i) Robertson, R. C.; Leitch, A. A.; Cvrkalj, K.; Reed, R. W.; Myles, D. J. T.; Dube, P. A.; Oakley, R. T. *J. Am. Chem. Soc.* **2008**, *130*, 14791–14801. (j) Robertson, R. C.; Leitch, A. A.; Cvrkalj, K.; Reed, R. W.; Myles, D. J. T.; Dube, P. A.; Oakley, R. T. *J. Am. Chem. Soc.* **2008**, *130*, 8414–8425. (k) Shuvaev, K. V.; Decken, A.; Grein, F.; Abeldin, T. M. S.; Thompson, L. K.; Passmore, J. *Dalton Trans.* **2008**, 4029–4037.(l) Rawson, J. M., Alberola, A. In *Handbook of Chalcogen Chemistry. New Perspectives in Sulfur, Selenium and Tellurium*; Devillanova, F., Ed.; RSC Press: Cambridge, U.K., 2007. (m) Robertson, C. M.; Myles, D. J. T.; Leitch, A. A.; Reed, R. W.; Dooley, B. M.; Frank, N. L.; Dube, P. A.; Thompson, L. K.; Oakley, R. T. *J. Am. Chem. Soc.* **2007**, *129*, 12688–12689. (n) Saito, G.; Yoshida, Y. *Bull. Chem. Soc. Jpn.* **2007**, *80*, 1–137. (o) Preuss, K. E. *Dalton Trans.* **2007**, 2357–2369. (p) Awaga, K.; Tanaka, T.; Shirai, T.; Umezono, Y.; Fujita, W. *C. R. Chim.* **2007**, *10*, 52–57. (q) Leitch, A. A.; Brusso, J. L.; Cvrkalj, K.; Reed, R. W.; Robertson, C. M.; Dube, P. A.; Oakley, R. T. *Chem. Commun.* **2007**, 3368–3370. (r) Leitch, A. A.; Reed, R. W.; Robertson, C. M.; Britten, J. F.; Yu, X.; Secco, R. A.; Oakley, R. T. *J. Am. Chem. Soc.* **2007**, *129*, 7903–7914. (s) Brusso, J. L.; Cvrkalj, K.; Leitch, A. A.; Oakley, R. T.; Reed, R. W.; Robertson, C. M. *J. Am. Chem. Soc.* **2006**, *128*, 15050–15081. (t) Rawson, J. M.; Alberola, A.; Whalley, A. *J. Mater. Chem.* **2006**, *16*, 2560–2575. (u) Cameron, T. S.; Decken, A.; Kowalczyk, R. M.; McInnes, E. J. L.; Passmore, J.; Rawson, J. M.; Shuvaev, K. V.; Thompson, L. K. *Chem. Commun.* **2006**, 2277–2279. (v) Decken, A.; Matar, S. M.; Passmore, J.; Shuvaev, K. V.; Thompson, L. K. *Inorg. Chem.* **2006**, *45*, 3878–3886. (w) Cameron, T. S.; Lemaire, M. T.; Passmore, J.; Rawson, J. M.; Shuvaev, K. V.; Thompson, L. K. *Inorg. Chem.* **2005**, *44*, 2576–2578.

(11) Currently, main group chemistry and materials science dealing with heavier chalcogens attract much attention. Of special interest are the interchalcogen interactions. Despite relative weakness, these interactions, for example, Se···S, both intra- and intermolecular, primary and secondary, play a unique role in physical, chemical, and biological processes, including, in particular, transfer of chiral information in chemical reactions. For selected recent work, see: (a) Gamez, G. A.; Yanez, M. *Chem. Commun.* **2011**, DOI: 10.1039/C0CC04675B. (b) Makherjee, A. J.; Zade, S. S.; Singh, H. B.; Suno, R. B. *Chem. Rev.* **2010**, *110*, 4357–4416.(c) In *Handbook of Chalcogen Chemistry. New Perspectives in Sulfur, Selenium and Tellurium*; Devillanova, F., Ed.; RSC Press: Cambridge, U.K., 2007. (d) Bleiholder, C.; Werz, D. B.; Koeppel, H.; Gleiter, R. *J. Am. Chem. Soc.* **2006**, *128*, 2666–2674. (e) Roy, D.; Sunoj, R. B. *J. Phys. Chem. A* **2006**, *110*, 5942–5947. (f) Tiecco, M.; Testaferri, L.; Santi, C.; Tomassini, C.; Santoro, S.; Marini, F.; Bagnoli, L.; Temperini, A.; Constantino, F. *Eur. J. Org. Chem.* **2006**, 4867–4873. (g) Bachrach, S. M.; Demoin, D. W.; Luk, M.; Miller, J. V. *J. Phys. Chem. A* **2004**, *108*, 4040–4046. (h) Tiecco, M.; Testaferri, L.; Santi, C.; Tomassini, C.; Marini, F.; Bagnoli, L.; Temperini, A. *Angew. Chem., Int. Ed.* **2003**, *42*, 3131–3133. (i) Tiecco, M.; Testaferri, L.; Santi, C.; Tomassini, C.; Marini, F.; Bagnoli, L.; Temperini, A. *Chem.—Eur. J.* **2002**, *8*, 1118–1124. (j) Vargas-Baca, I.; Chivers, T. *Phosphorus Sulfur Silicon Relat. Elem.* **2000**, *164*, 207–227.

(12) (a) Zibarev, A. V.; Mews, R. In *Frontiers of Selenium and Tellurium Chemistry: From Small Molecules to Biomolecules and Materials*; Laitinen, R. S., Woollins, J. D., Eds.; Springer: New York, 2011; in press. (b) Vasilieva, N. V.; Irtegova, I. G.; Gritsan, N. P.; Lonchakov, A. V.; Makarov, A. Yu.; Shundrin, L. A.; Zibarev, A. V. *J. Phys. Org. Chem.* **2010**, *23*, 536–543.(c) Gritsan, N. P.; Suturina, E. A.; Semenov N. A.; Lonchakov, A. V.; Zibarev, A. V. Work in progress.

(13) (a) Hanson, P. *Adv. Heterocycl. Chem.* **1980**, *27*, 31–149. (b) Kwan, C. L.; Carmack, M.; Kochi, J. K. *J. Phys. Chem.* **1976**, *80*, 1786–1792. (c) Kamiya, M.; Akahori, Y. *Bull. Chem. Soc. Jpn.* **1970**, *43*, 268–271. (d) Atherton, N. M.; Ockwell, J. N.; Dietz, R. *J. Chem. Soc. A* **1967**, 771–777.

(14) Konchenko, S. N.; Gritsan, N. P.; Lonchakov, A. V.; Radius, U.; Zibarev, A. V. *Mendeleev Commun.* **2009**, *19*, 7–9.

(15) (a) Semenov, N. A.; Pushkarevsky, N. A.; Lonchakov, A. V.; Bogomyakov, A. S.; Pritchina, E. A.; Suturina, E. A.; Gritsan, N. P.; Konchenko, S. N.; Mews, R.; Ovcharenko, V. I.; Zibarev, A. V. *Inorg. Chem.* **2010**, *49*, 7558–7564. (b) Konchenko, S. N.; Gritsan, N. P.; Lonchakov, A. V.; Irtegova, I. G.; Mews, R.; Ovcharenko, V. I.; Radius, U.; Zibarev, A. V. *Eur. J. Inorg. Chem.* **2008**, 3833–3838.

(16) Gritsan, N. P.; Lonchakov, A. V.; Lork, E.; Mews, R.; Pritchina, E. A.; Zibarev, A. V. *Eur. J. Inorg. Chem.* **2008**, 1994–1998.

(17) (a) Bagryanskaya, I. Yu.; Gatilov, Yu. V.; Gritsan, N. P.; Ikorskii, V. N.; Irtegova, I. G.; Lonchakov, A. V.; Lork, E.; Mews, R.; Ovcharenko, V. I.; Semenov, N. A.; Vasilieva, N. V.; Zibarev, A. V. *Eur. J. Inorg. Chem.* **2007**, 4751–4761. (b) Ikorskii, V. N.; Irtegova, I. G.; Lork, E.; Makarov, A. Yu.; Mews, R.; Ovcharenko, V. I.; Zibarev, A. V. *Eur. J. Inorg. Chem.* **2006**, 3061–3067. (c) Makarov, A.Yu.; Irtegova, I. G.; Vasilieva, N. V.; Bagryanskaya, I. Yu.; Borrmann, T.; Gatilov, Yu. V.; Lork, E.; Mews, R.; Stohrer, W.-D.; Zibarev, A. V. *Inorg. Chem.* **2005**, *44*, 7194–7199.

(18) (a) Emge, T. J.; Romanelly, M. D.; Moore, B. F.; Brennan, J. G. *Inorg. Chem.* **2010**, *49*, 7304–7312. (b) Fuller, A. L.; Knight, F. R.; Slawin, A. M. Z.; Woollins, J. D. *Eur. J. Inorg. Chem.* **2010**, 4034–4043. (c) Eichhoefer, A.; Wood, P. T.; Viswanath, R.; Mole, R. A. *Eur. J. Inorg. Chem.* **2007**, 4794–4799.(d) Gimeno, M. C. In *Handbook of Chalcogen Chemistry. New Perspectives in Sulfur, Selenium and Tellurium*; Devillanova, F., Ed.; RSC Press: Cambridge, U.K., 2007. (e) Sadekov, I. D.; Minkin, V. I. *J. Sulfur Chem.* **1997**, *19*, 285–348.

(19) (a) Stuzhin, P. A.; Bauer, E. M.; Ercolani, C. *Inorg. Chem.* **1999**, *37*, 1533–1539. (b) Bauer, E. M.; Ercolani, C.; Galli, P.; Popkova, I. A.; Stuzhin, P. A. *J. Porphyrins Phthalocyanines* **1999**, *3*, 371–379.

(20) Duling, D. R. *J. Magn. Reson.* **1994**, *104*, 105–110.

(21) Sheldrick, G. M. *Acta Crystallogr. A* **2008**, *64*, 112–122.

(22) (a) Spek, A. L. *PLATON program, A Multipurpose Crystallographic Tool*, version 1.15; Utrecht University: Utrecht, The Netherlands, 2008. (b) Spek, A. L. *J. Appl. Crystallogr.* **2003**, *36*, 7–17.

(23) (a) Becke, A. D. *J. Chem. Phys.* **1993**, *98*, 5648–5652. (b) Lee, C.; Yang, W.; Parr, R. G. *Phys. Rev. B* **1988**, *37*, 785–789.

(24) Blockhuys, F. In *Computational Methods in Science and Engineering. Advances in Computational Science*; Maroulis, G., Simos, T. E., Eds.; American Institute of Physics: Woodbury, NY, 2009; Vol. 1.

(25) Zhao, Y.; Truhlar, D. G. *Theor. Chem. Acc.* **2008**, *120*, 215–241.

(26) Grimme, S. *J. Comput. Chem.* **2006**, *27*, 1787–1799.

(27) (a) Schafer, A.; Horn, H.; Ahlrichs, R. *J. Chem. Phys.* **1992**, *97*, 2571–2577. (b) Weigend, F.; Ahlrichs, R. *Phys. Chem. Chem. Phys.* **2005**, *7*, 3297–3305. (c) Weigend, F. *Phys. Chem. Chem. Phys.* **2006**, *8*, 1057–1065.

(28) Dreuw, A.; Head-Gordon, M. *Chem. Rev.* **2005**, *105*, 4009–4037.

(29) (a) Zhao, Y.; Truhlar, D. G. *J. Phys. Chem. A* **2006**, *110*, 13126–13130. (b) Zhao, Y.; Truhlar, D. G. *Acc. Chem. Res.* **2008**, *41*, 157–167.

(30) Frisch, M. J.; *Gaussian 09*, Revision A.1; Gaussian Inc.: Wallingford, CT, 2009 (full reference available in the Supporting Information).

(31) (a) Tomasi, J.; Mennucci, B.; Cammi, R. *Chem. Rev.* **2005**, *105*, 2999–3093. (b) Barove, V.; Polimeno, A. *Chem. Soc. Rev.* **2007**, *36*, 1724–1731.

(32) Marenich, A. V.; Cramer, C. J.; Truhlar, D. G. *J. Phys. Chem. B* **2009**, *113*, 6378–6396.

(33) Keith, T. A. *AIMAll*, Version 10.03.25; aim.tkgristll.com.

(34) (a) Lee, L. M.; Elder, P. J. W.; Cozzolino, A. F.; Yang, Q.; Vargas-Baca, I. *Main Group Chem.* **2010**, *9*, 117–133. (b) Cozzolino, A. F.; Bain, A. D.; Hanhan, S.; Vargas-Baca, I. *Chem. Commun.* **2009**, 4043–4045. (c) Risto, M.; Reed, R. W.; Robertson, C. M.; Oilunkaniemi, R.; Laitinen, R. S.; Oakley, R. T. *Chem. Commun.* **2008**, 3278–3280. (d) Nunn, A. J.; Ralph, J. T. *J. Chem. Soc. C* **1966**, 1568–1570.

(35) Lork, E.; Mews, R.; Zibarev, A. V. *Mendeleev Commun.* **2009**, *19*, 147–148.

(36) (a) Cordero, B.; Gomez, V.; Platero-Prats, A. E.; Reves, M.; Echeverria, J.; Cremades, E.; Barragan, F.; Alvarez, S. *Dalton Trans.* **2008**, 2832–2838.

(37) (a) Rowland, R. S.; Taylor, R. *J. Phys. Chem.* **1996**, *100*, 7384–7391. (b) Bondi, A. *J. Phys. Chem.* **1964**, *68*, 441–451.

(38) (a) Kumar, S.; Panda, S.; Singh, H. B.; Woltmershaeuser, G.; Butcher, R. J. *Struct. Chem.* **2007**, *18*, 127–132. (b) Mugesh, G.; du Mont, W.-W.; Wismach, C.; Jones, P. G. *ChemBioChem* **2002**, *3*, 440–447. (c) Neugebauer, D.; Schubert, U. *J. Organomet. Chem.* **1983**, *256*, 43–46.

(39) (a) Atanassov, P. K.; Linden, A.; Heimgartner, H. *J. Sulfur Chem.* **2006**, *27*, 181–191. (b) Billing, D. G.; Levendis, D. C.; Reid, D. H. *Acta Crystallogr. C* **1991**, *47*, 759–761. (c) Allen, C.; Boeyens, J. C. A.; Briggs, A. G.; Denner, L.; Markwell, A. J.; Reid, D. H.; Rose, B. G. *Chem. Commun.* **1987**, 967–968.

(40) (a) Chidambaram, S. P.; Aravamudan, G.; Seshasayee, M. *Z. Kristallogr.* **1989**, *187*, 231–233. (b) Husebye, S.; Maartmann-Moe, K. *Acta Chem. Scand. A* **1983**, *37*, 219–225. (c) Anderson, O. P.; Husebye, S. *Acta Chem. Scand.* **1970**, *24*, 3141–3150.

(41) Trofimov, B. A.; Sinegovskaya, L. M.; Gusarova, N. K. *J. Sulfur Chem.* **2009**, *30*, 518–554.

(42) (a) Riley, K.; Pitonak, M.; Jurecka, P.; Hobza, P. *Chem. Rev.* **2010**, *110*, 5023–5053. (b) Kannemann, F. O.; Becke, A. D. *J. Chem. Theory Comput.* **2010**, *6*, 1081–1088. (c) Sherrill, C. D.; Takatani, T.; Hohenstein, E. G. *J. Phys. Chem. A* **2009**, *113*, 10146–10159. (d) Johnson, E. R.; Mackie, I. D.; DiLabio, G. A. *J. Phys. Org. Chem.* **2009**, *22*, 1127–1135.

(43) (a) Cozzolino, A. F.; Yang, Q.; Vargas-Baca, I. *Cryst. Growth Des.* **2010**, *10*, 4959–4964.(b) Semenov, N. A.; Pushkarevsky, N. A.; Beckmann, J.; Lork, E.; Mews, R.; Zibarev, A. V. Work in progress (3,4-dicyano-1,2,5-telluradizole, its 1:2 complex with pyridine, and pyridinium and triethylammonium salts of 1-X-3,4-dicyano-1,2,5-telluradiazolide and 1,1-X_2-3,4-dicyano-1,2,5-telluradiazolide (X = Cl, Br) anions are prepared and characterized by XRD).

(44) (a) In *The Quantum Theory of Atoms in Molecules*; Motta, C. F., Boid, R. J., Eds.; Wiley: Weinheim, 2007. (b) Bader, R. F. W. *Monatsh. Chem.* **2005**, *136*, 819–856.(c) Bader, R. F. W. *Atoms in Molecules: A Quantum Theory*; Oxford University Press: Oxford, 1990.

(45) (a) Reed, A. E.; Curtiss, L. A.; Weinhold, F. *Chem. Rev.* **1988**, *88*, 899–926.(b) Weinhold, F.; Landis, C. R. *Valency and Bonding: A Natural Bond Orbital Donor-Acceptor Perspective*; Cambridge University Press: Cambridge, U.K., 2005.

(46) (a) Iwaoka, M.; Katsuda, T.; Kamatsu, H.; Tomada, S. *J. Org. Chem.* **2005**, *70*, 321–327. (b) Iwaoka, M.; Komatsu, H.; Katsuda, T.; Tomada, S. *J. Am. Chem. Soc.* **2004**, *126*, 5309–5317.

(47) (a) Besler, B. H.; Merz, K. M.; Kollmann, P. A. *J. Comput. Chem.* **1990**, *11*, 431–439. (b) Singh, U. C.; Kollman, P. A. *J. Comput. Chem.* **1984**, *5*, 129–145.

(48) (a) Barbara, P. F.; Meyer, T. J.; Ratner, M. A. *J. Phys. Chem.* **1996**, *100*, 13148–13168.(b) In *Electron Transfer in Inorganic, Organic, and Biological Systems*; Bolton, J. R., Mataga, N., McLendon, G., Eds.; Advances in Chemistry Series; American Chemical Society: Washington DC, 1991. (c) Marcus, R. A. *J. Chem. Phys.* **1956**, *24*, 966–978.